Childs Nerv Syst
DOI 10.1007/s00381-015-2947-4

ORIGINAL PAPER

Association between the growth rate of subependymal giant cell astrocytoma and age in patients with tuberous sclerosis complex

Jeng-Dau Tsai[1,2] · Chang-Ching Wei[3,4] · Teng-Fu Tsao[1,5] · Yu-Ping Hsiao[1,6] · Henry J. Tsai[7] · Sheng-Hui Yang[8] · Min-Ling Tsai[1,9] · Ji-Nan Sheu[1,2]

Received: 1 October 2015 / Accepted: 27 October 2015

Abstract
Purpose The most common neurological complications associated with tuberous sclerosis complex (TSC) include intractable seizures that begin in infancy and subependymal giant cell astrocytoma (SEGA) complicated by hydrocephalus with increasing age. Information on SEGA growth of TSC patients is limited. This study aimed to examine the TSC-SEGA growth rates by periodic neuroimaging.
Methods This study evaluated the TSC-SEGA growth rates by serial neuroimaging. Fifty-eight patients with TSC underwent systematic evaluation, including a review of medical history and serial brain neuroimaging.
Results While magnetic resonance imaging was more sensitive in detecting cortical tubers than computed tomography (73.1 vs. 0 %, $p<0.001$), its efficacy in identifying intracranial lesions was comparable to that of computed tomography (96.2 vs. 100 %, $p=0.658$). Significant tumor growth was observed in children ($p=0.012$) and adults ($p=0.028$) during follow-up periods, respectively (median for children 23.5 months, interquartile range 18–40 months and median for adults 23 months, interquartile range 12–34 months). Further, the SEGA growth rate in children was significantly higher than that in adults (75.6 vs. 16.5 %, $p=0.03$).
Conclusions The results of the study show that SEGA has a significantly higher growth rate in children using serial follow-up brain imaging, suggesting the importance of performing follow-up neuroimaging at yearly intervals in childhood to identify and prevent potential comorbidities.

Keywords Tuberous sclerosis complex · Subependymal giant cell astrocytoma · Neuroimaging · Magnetic resonance imaging

✉ Ji-Nan Sheu
cshy098@csh.org.tw

1 School of Medicine, Chung Shan Medical University, No. 110, Section 1, Jianguo North Road, Taichung 402, Taiwan

2 Department of Pediatrics, Chung Shan Medical University Hospital, No. 110, Section 1, Jianguo North Road, Taichung 402, Taiwan

3 Children's Hospital, China Medical University Hospital, Taichung, Taiwan

4 School of Medicine, China Medical University, Taichung, Taiwan

5 Department of Medical Imaging, Chung Shan Medical University Hospital, Taichung, Taiwan

6 Department of Dermatology, Chung Shan Medical University Hospital, Taichung, Taiwan

7 Department of Health and Nutrition Biotechnology, Asia University, Taichung, Taiwan

8 Department of Life Sciences, National Chung Hsing University, Taichung, Taiwan

9 Department of Pharmacy, Chung Shan Medical University Hospital, Taichung, Taiwan

Introduction

Tuberous sclerosis complex (TSC) is a rare and slowly progressive genetic disorder characterized by benign tumors in multiple organs, with diverse clinical manifestations in affected individuals [1–3]. The common symptoms of TSC include seizures, mental retardation, and facial angiofibromas, as noted by Vogt in 1908 [4]. Neurological symptoms of TSC are attributable to the involvement of the brain and account for the initial clinical presentations and the most severe manifestations of TSC [5–7]. Intractable seizures along with evidence of intracranial lesions during infancy prompt clinical diagnosis of TSC. These neurological comorbidities usually are a

Published online: 09 November 2015

huge psychological burden to caregivers because of the lifelong course of the treatment [8, 9].

Obstructive hydrocephalus is quite common during childhood and generally develops in all patients with subependymal giant cell astrocytoma (SEGA) [10]. SEGA may grow with or without associated clinical symptoms, leading to potential intracranial lesions and subsequent hydrocephalus with age. With the development of neuroimaging techniques, clinicians can visualize intracranial tubers or subependymal nodules during initial evaluation and ongoing surveillance. Advances in medical information and imaging techniques can help identify and examine the involved organs, without tissue biopsy [11, 12]. Optimal outcome is associated with early detection and follow-up; hence, patients should be regularly monitored via magnetic resonance imaging (MRI).

Because information on SEGA growth of TSC patients is limited, clinical follow-up and neuroimaging may be needed to minimize the neuropsychological burden. Therefore, this study aimed to examine the neurological aspects of TSC, including neuroimaging of intracranial lesions and SEGA growth rates from childhood to adulthood.

Materials and methods

Patients

Patients diagnosed with TSC were systematically evaluated from 2009 to 2013 at the integrated clinics for TSC at a single medical center. All patient diagnoses were confirmed using the Roach's Clinical Diagnostic Criteria and the 2012 International TSC Consensus Conference Guidelines [12]. The subjects were either previously evaluated at integrated clinics or referred by the Taiwan Tuberous Sclerosis Complex (TTSC, http://www.ttsc.org.tw/) for medical consultation. The institutional review board approved this study (CS12245). The parents of all the participants provided informed consent.

During their visit to the integrated clinics, patients underwent a systematic evaluation and questionnaire interview, including a medical review of epilepsy history and a neurobehavioral disorder assessment. Seizure remission was defined as no seizure for 5 years or longer with or without anticonvulsant treatment at the time of ascertainment. Seizure-free state was defined as a period of no seizures lasting 2 to 5 years without anticonvulsant treatment. Neurobehavioral comorbidities, including mental retardation or autism spectrum disorder, were assessed by clinical psychologists using the Wechsler Intelligence Scale or the Childhood Autism Rating Scale, respectively.

The patients were routinely evaluated using brain MRI or computed tomography (CT) scanning. SEGAs were defined as hamartomas arising at the caudothalamic groove adjacent to the foramen of Monro [12]. Subependymal nodules (SENs) were defined as small asymptomatic protrusions into the walls of the lateral ventricles [9, 12]. Based on axial MRI or CT imaging, manual volumetric methods for regions of interest were performed for measuring SEGA size.

CT scan examination

CT scan examinations were performed using a 40-slice scanner (Brilliance 40, Philips, Israel) or a 320-slice scanner (Toshiba Aquilion ONE, Toshiba Medical Systems, Otawara, Japan) with 80–120 kVp of the X-ray tube potential. The tube current was set according to the patient's size or body weight to obtain an acceptable radiographic optical density and patient dose. The projection data of the initial CT product was reconstructed into axial and coronal images with 3.0–4.0 mm of slice thickness.

Suitable sedation for neonates and younger children was achieved with rectal chloral hydrate, administered dosage according to the patient's body weight and the clinical condition. Sedation were not achieved for older children or adults. Contrast media was used if indicated.

MRI examination

MRI examinations were performed with 1.5-T scanner (Magnetom Sonata, Siemens Medical Solutions, Erlangen, Germany, or Signa Horizon Echospeed, General Electric Medical Systems, Milwaukee, WI, USA), equipped with high-performance three-axis gradient systems. The scan protocol included T1-weighted, T2-weighted, fluid attenuation inversion recovery and diffusion-weighted imaging. Contrast-enhanced MR imaging was used if indicated. Typically, T1-weighted images were used for volume assessment. Imaging parameters for this sequence were as follows: TR/TE=400–500/13 ms, 4.0 or 5.0-mm slice thickness, field of view=170–230 mm.

Baseline volumes were calculated; each volume was treated as an ellipsoid, according to the volume equation=$(4/3\times\pi\times a\times b\times c)$, with a, b, and c, representing the respective three-dimensional radii (cm) of the lesions in question. The total volumes were calculated as the sum of each section (all in-section volumes).

Statistical analysis

Correlations between lesion size and patient age were determined using the Wilcoxon signed-rank test and the Spearman rank correlation coefficient. Non-parametric data were assessed by the Mann-Whitney U test and expressed as medians and interquartile ranges (IQR [Q_1–Q_3]). Chi-squared test or Fisher's exact test was used to compare categorical variables. Statistical significance was set at $p<0.05$. All statistical analyses were conducted using SPSS for Windows, Version 14.0 (SPSS Inc., Chicago, IL).

Table 1 Neurological comorbidities in patients with TSC (n=58)

Characteristic	All n (%)	Children (<18 years)	Adults (≥18 years)	p
Number of patients	58	33	25	
Sex (male/female)	23/35	15/18	8/17	0.300
Brain lesions				
SEGA	26 (44.8)	17 (51.5)	9 (36.0)	0.239
Maximal diameter (cm)				
0.5–1	17 (29.3)	12 (36.4)	5 (20.0)	0.365
≥1	9 (15.5)	5 (15.2)	4 (16.0)	
Hydrocephalus	5 (8.6)	3 (9.1)	2 (8.0)	0.792
Cortical tubers	44/54 (81.5)	27/31 (87.1)	17/23 (73.9)	0.189
SENs	48 (82.8)	28 (84.8)	20 (80.0)	0.731
Neurobehavioral disorders	28 (48.3)	21 (63.6)	6 (24.0)	0.003
Seizures	45 (77.6)	28 (84.8)	17 (68.0)	0.128
Active	28 (62.2)	20 (71.4)	8 (32.0)	0.025
Remission/free	17 (37.8)	8 (24.2)	9 (36.0)	0.495

Neurobehavioral included mental retardation and autistic spectrum

SEGA subependymal giant cell astrocytoma, *SENs* subependymal nodules

Results

Fifty-eight patients (23 males and 35 females; 1 month to 68 years of age) were enrolled. Cortical tubers and SENs were detected in 44/54 (81.5 %) and 48 (82.8 %) patients using MRI and CT, respectively. The incidence of SEGA was 15.2 % (5/33) in childhood and 16.0 % (4/25) in adulthood, respectively (lesion diameter at >1.0 cm). Of those patients, five (8.6 %) suffered from hydrocephalus and received tumor resection, including three children (9.1 %) and two adults (8.0 %) (p=0.792). Neurobehavioral disorders (i.e., mental retardation and autism) and seizure history were recorded in 28 (48.3 %) and 45 (77.6 %) patients, respectively. Of the patients with a history of seizures, 17 (37.8 %) experienced seizure remission (Table 1). Comparison of the clinical features of children (age <18 years) with those of adults (age ≥18 years) did not reveal statistical differences between the number of children and adults with SEGA, cortical tubers, and SENs. The rate of neurobehavioral comorbidities was significantly higher in children than that in adults (63.6 vs. 24.0 %, p=0.003).

For intracranial lesion detection, 52 of the 58 patients were examined by MRI and 12 by CT (Table 2). The follow-up period ranged from 10 to 71 months (median=24 months). Intracranial calcifications were detected using CT (p<0.001), while cortical tubers were confirmed using MRI (p<0.001). Because the sensitivity of CT was comparable to that of MRI in detecting SEGAs (p=0.675), CT was considered to be an alternative for intracranial tumor identification, particularly for patients who could not tolerate MRI examinations.

A correlation between SEGA volume (in cm^3) and patient age is shown in Fig. 1; SEGA volumes remained stable around 1.0 cm^3 in children but increased to >1.0 cm^3 in adults. Sixteen patients (nine children and seven adults) were evaluated by follow-up brain MRI (Table 3). In children, significant tumor growth was observed (median size 0.25 cm^3, range 0.23–0.71 cm^3 vs. median size 0.41 cm^3, range 0.28–0.85 cm^3; p=0.012) during the follow-up period (median 23.5 months; IQR 18–40 months). An example of Fig. 2 illustrated a boy with TSC1 mutation and a SEGA (0.55 cm in diameter) at the age of 3 years; the tumor size progressed to 1.45 cm in diameter on the follow-up MRI at the age of 7 years. Similar results were observed in adults (median size 0.20 cm^3, range 0.12–2.93 cm^3 vs. median size 0.25 cm^3, range 0.15–3.38 cm^3; p=0.028) during the follow-up period (median 23 months; IQR 12–34 months). Further, comparison

Table 2 Comparison of MRI and CT for identifying intracranial lesions in patients with TSC (n=58)

Variable	MRI n (%)	CT	p
Number	52	12	
Cortical tubers	38 (73.1)	0 (0)	<0.001
SENs	42 (80.8)	12 (100.0)	0.104
SEGA	30 (58.0)	7 (58.3)	0.675
Calcification	0 (0)	12 (100.0)	<0.001
All	50 (96.2)	12 (100.0)	0.658

SEGA subependymal giant cell astrocytoma, *SENs* subependymal nodules, *CT* computed tomography, *MRI* magnetic resonance imaging

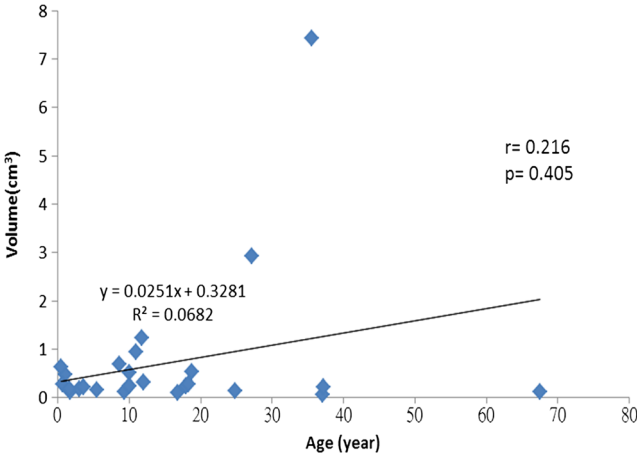

Fig. 1 Correlation between patient age and the volume of subependymal giant cell astrocytoma (r=0.216; p=0.405)

of the SEGA growth rate between children and adult revealed that the SEGA growth rates in children were significantly higher than that in adults, with a median of 75.6 % in children (range 6.3–201.3 %) versus a median of 16.5 % in adults (range 3.5–37.7 %, p=0.03; Fig. 3).

Discussion

These results highlight the importance of follow-up evaluations for patients with neurological abnormalities, particularly in determining SEGA growth using neuroimaging in children and adults. The current study shows the more rapid growth rate of SEGA in childhood than that in adulthood. It implies that the annual follow-up of neuroimaging in childhood is crucial to minimize TSC-SEGA associated with comorbidities and complications. In the study, five patients received operation due to the progression of their tumor size causing hydrocephalus on the follow-up neuroimaging. Thus, TSC-SEGA-associated risks can be minimized by early diagnosis, lifelong monitoring, and medical treatment [13, 14]. Our study may provide the information regarding monitoring the progression of SEGAs in the high-risk population for clinicians on the neurosurgical clinical practice.

To the best of our knowledge, this is the first study to clarify the different prevalence of TSC-SEGA by different definition of tumor size and to compare the growth rates between the different age groups. The definition of SEGAs is varied in size and results in different prevalence. Roth et al. [15] defined SEGA as either a lesion (diameter >1.0 cm) at the caudothalamic groove in any direction or a subependymal lesion at any location with serial growth occurring during consecutive imaging regardless of size. Jóźwiak et al. [16] defined SEGA in a patient with TSC as a tumor (>0.5 cm in diameter) that is typically localized near the foramen of Monro, with documented growth and gadolinium enhancement during neuroimaging. The high SEGA prevalence based on diameter >0.5 cm in the current study can be partly explained by the different definitions of SEGA size and the routine MRI performed as a strategy for managing TSC patients. This suggests that high-resolution imaging of small lesions may lead to a higher identification rate [17]. Adriaensen et al. [18] reported the occurrence of SEGA in 20 % of TSC patients as analyzed by CT (average 11.4 mm; range 4–29 mm), whereas Goh et al. [19] reported SEGA incidence in 8.2 % of TSC patients who underwent surgical SEGA resection with pathological confirmation. In the current study, most of the patients were referred for medical consultation without emergency surgical conditions, which may have resulted in the small SEGA size detected in this study compared to those observed in previous studies. However, this may also be a consequence of selection bias.

The revised diagnostic criteria for TSC depend on clinical presentations or genetic confirmation, indicating that pathological evidence is not necessary for physicians [9–12]. Currently, MRI is considered as the detection method of choice for evaluating the brains of patients suspected to have or diagnosed with TSC [7, 11] since hamartomas and gliotic areas, especially cortical tubers, are visible on MRI scans [20]. CT readily depicts calcified cortical tubers and calcified SENs, which tend to calcify over time, causing them to appear as periventricular calcifications [21]. Yates et al. [22] compared

Table 3 Growth rates of SEGA in different age groups of TSC patients

Volume (cm^3)	N	First imaging		Second imaging		Duration (month)		p^a
		Median	IQR	Median	IQR	Median	IQR	
All	14	0.24	0.15–0.95	0.34	0.27–1.15	23	17–36	0.001
Children (<18 years)	9	0.25	0.23–0.71	0.41	0.28–0.85	23.5	18–40	0.012
Adults (≥18 years)	7	0.20	0.12–2.93	0.25	0.15–3.38	23	12–34	0.028

IQR interquartile range

[a] Wilcoxon signed-rank test

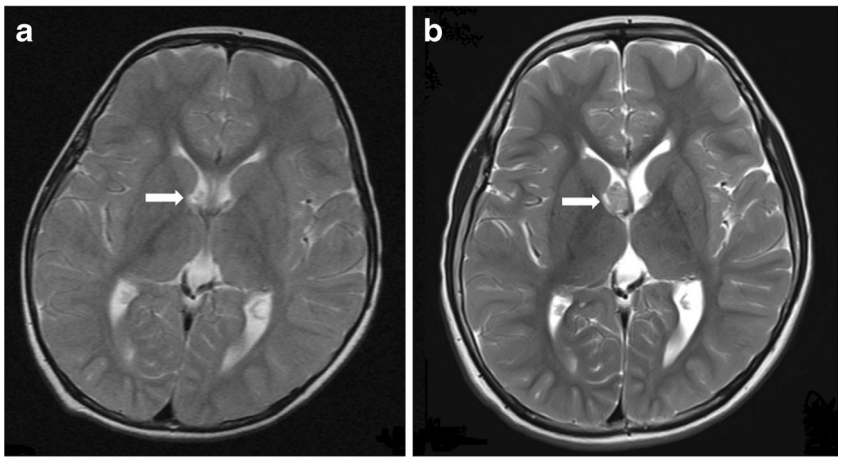

Fig. 2 **a** MRI of the brain in a 3-year-old boy with TSC1 mutation showed a subependymal giant cell astrocytoma with 0.55 cm in diameter (*white arrow*). **b** A follow-up MRI at the age of 7 years revealed the progression of tumor size to 1.45 cm in diameter (*white arrow*)

the detection rates of MRI with CT for cortical tubers/SENs/SEGAs; it showed preferable results of MRI because of better visualization of cortical tubers. Cortical tubers can be seen as low-attenuating peripheral lesions on CT scans but are more easily identified with MRI. It is recommended performing routine brain MRI to assess the presence of cortical tubers/SENs/SEGAs. However, brain CT still has its role in neuroimaging survey of TSC. Brain CT may be used instead of MRI in the following situations, including unavailability of MRI in radiological departments and the use of CT as an urgent diagnostic tool for acute hydrocephalus [23]. In all other circumstances, radiation exposure due to CT imaging should be avoided.

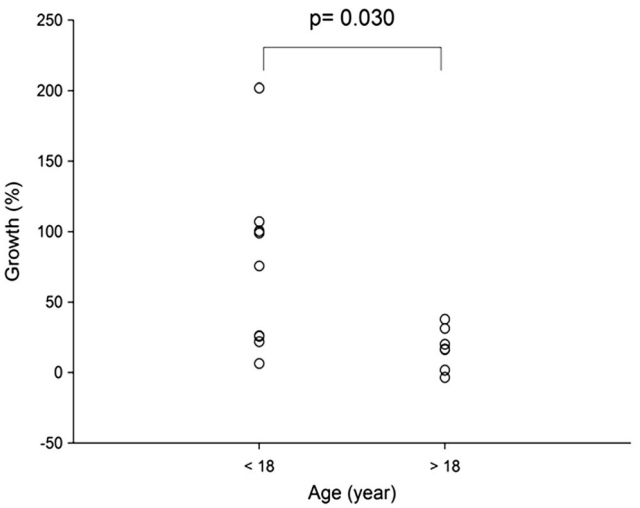

< 18 y/o (N=9)		> 18 y/o (N=7)	
Median (%)	IQR	Median (%)	IQR
75.6	23.6-103.6	16.5	1.6-31.2

†Mann-Whitney U test
IQR= Interquartile range, *p<0.05

Fig. 3 Trends of subependymal giant cell astrocytoma growth rates in different age groups. The growth rates in children (<18 years of age; $n=9$) were significantly different from the growth rates in adults (≥18 years of age; $n=7$) ($p=0.03$). *IQR* interquartile range; *$p<0.05$

SEGAs and SENs have similar histopathological features but differ in their location and growth rates. For location, SEGAs are typically located at the caudothalamic groove, as opposed to SENs, which are located in the ependymal lining of the lateral ventricles along the caudate nucleus. For growth rates, one major difference between SEGAs and SENs is the serial growth associated with SEGAs, whereas SENs remain stable in size [19]. For SENs and SEGAs, the protruding characteristics over the periventricular area can be identified by either MRI or CT [24, 25].

The consensus guideline for TSC brain screening suggests that brain MRIs should be performed periodically in patients with asymptomatic TSC to monitor new SEGA occurrence. Follow-up evaluations of SEGAs are recommended for patients with large or growing SEGAs or with SEGA-related subsequent asymptomatic ventriculomegaly; these patients should undergo MRI examination more frequently [14, 19]. The recent studies have shown that new SEGAs very rarely arise after 20–25 years of age, suggesting that monitoring of SEGA growth should be performed every 2 years before the age of 20 years [18]. Hence, individuals without SEGAs by the age 25 years do not need continuous surveillance imaging. However, children with asymptomatic SEGAs should continue to be monitored by imaging for the possibility of growth. Because of lack of knowledge regarding SEGA growth beyond 25 years of age, follow-up MRIs may be prolonged in the presence of a stable condition [15]. A limited number of studies have evaluated SEGAs via serial imaging and calculated TSC-SEGA growth rates. In the current study, SEGA volumes remained <1.0 cm^3 in childhood but tended to be larger during adulthood. On the contrary, the SEGA growth rate in children was significantly higher than that in adults, indicating the importance of periodic follow-ups. The current results highlight the importance of annual screenings in childhood to monitor potential SEGA-related comorbidities.

Generally, SEGA usually grow slowly, but significant increase in tumor size can be observed in 1–2-year-long follow-up. It has been shown that in patient with TSC2 mutation, SEGA develop significantly more frequently and grow more rapidly in comparison to TSC1 mutation. Therefore, follow-up neuroimaging is recommended in patients with TSC2 mutation every 2 years and every 3 years in patients with TSC1 mutation [26]. Thus, integration with biomolecular data and a longer radiological follow-up are needed for monitoring the progression of SEGA in the high-risk patients.

The limitations of this study include its retrospective design, small sample size, variable follow-up durations, and variable age of the TSC population. All patients underwent brain MRI, but only a minority underwent follow-up imaging that may limit the study conclusions. The SEGA growth rate should be stratified according to patient age for assessment of neurobehavioral comorbidities. These may pose a selection bias. In the current study, most patients enrolled were diagnosed based on the clinical diagnostic criteria recommended by the 2012 International Tuberous Sclerosis Complex Consensus Conference [12]; thus, there were no enough biomolecular data to make analysis of the effect on the progression of SEGA between the TSC1 and TSC2 mutations. Lastly, the number of the reported cases may be too small to make a firm conclusion. Further prospective studies with larger cohorts are warranted.

In conclusion, the prevalence of SEGA varied owing to the different definitions of SEGA tumor size. CT and MRI equally identified TSC-associated intracranial lesions, but MRI was preferable for cortical tubes. SEGA growth rates in children were significantly higher than in adults using serial follow-up brain imaging, suggesting the importance of performing follow-up neuroimaging at a yearly interval for the high-risk group to identify and prevent potential comorbidities, especially in the pediatric patients.

Acknowledgments This work was supported by Chung Shan Medical University Hospital (CRDA001MIC03). Authors gratefully acknowledge the support of the Taiwan Tuberous Sclerosis Complex Association, the patients, and caregivers who participated in this survey.

Compliance with ethical standards

Conflict of interest The authors have no conflicts of interest to disclose.

References

1. Rieger E, Kerl H (1992) The clinical spectrum of organ manifestations of tuberous sclerosis. Hautarzt 43(5):272–277
2. Tan TK, Chen FL, Sheu JN, Chen SM, Huang HH, Tsai JD (2014) Tuberous sclerosis complex associated with heterotopic ossification in a young girl. Pediatr Neonatol 55(1):65–77
3. Tsai JD, Wei CC, Chen SM, Lue KH, Sheu JN (2014) Association between the growth rate of renal cysts/angiomyolipomas and age in the patients with tuberous sclerosis complex. Int Urol Nephrol 46(9):1685–1690
4. Jay V (1999) Historical contributions to pediatric pathology: legacy of Dr. Ewing. Pediatr Dev Pathol 2(6):597–599
5. Staley BA, Vail EA, Thiele EA (2011) Tuberous sclerosis complex: diagnostic challenges, presenting symptoms, and commonly missed signs. Pediatrics 127(1):e117–125
6. Franz DN, Bissler JJ, McCormack FX (2010) Tuberous sclerosis complex: neurological, renal and pulmonary manifestations. Neuropediatrics 41(5):199–208
7. Christophe C, Sékhara T, Rypens F, Ziereisen F, Christiaens F, Dan B (2000) MRI spectrum of cortical malformations in tuberous sclerosis complex. Brain Dev 22(8):487–493
8. Hallett L, Foster T, Liu Z, Blieden M, Valentim J (2011) Burden of disease and unmet needs in tuberous sclerosis complex with neurological manifestations: systematic review. Curr Med Res Opin 27(8):157–183
9. Rosser T, Panigrahy A, McClintock W (2006) The diverse clinical manifestations of tuberous sclerosis complex: a review. Semin Pediatr Neurol 13(1):27–36
10. Roach ES, Sparagana SP (2004) Diagnosis of tuberous sclerosis complex. J Child Neurol 19(9):643–649
11. Roach ES, Gomez MR, Northrup H (1998) Tuberous sclerosis complex consensus conference: revised clinical diagnostic criteria. J Child Neurol 13(12):624–628
12. Northrup H, Krueger DA, International Tuberous Sclerosis Complex Consensus Group (2013) Tuberous sclerosis complex diagnostic criteria update recommendations of the 2012 international tuberous sclerosis complex consensus conference. Pediatr Neurol 49(4):243–254
13. Wataya-Kaneda M, Tanaka M, Hamasaki T (2013) Trends in the prevalence of tuberous sclerosis complex manifestations: an epidemiological study of 166 Japanese patients. PLoS One 8(5):e63910
14. Krueger DA, Northrup H (2013) Tuberous sclerosis complex surveillance and management: recommendations of the 2012 International Tuberous Sclerosis Complex Consensus Conference. Pediatr Neurol 49(4):255–265
15. Roth J, Roach ES, Bartels U, Jóźwiak S, Koenig MK, Weiner HL et al (2013) Subependymal giant cell astrocytoma: diagnosis, screening, and treatment. Recommendations from the International Tuberous Sclerosis Complex Consensus Conference 2012. Pediatr Neurol 49(6):439–444
16. Jóźwiak S, Nabbout R, Curatolo P (2013) Management of subependymal giant cell astrocytoma (SEGA) associated with tuberous sclerosis complex (TSC): clinical recommendations. Eur J Paediatr Neurol 17(4):348–352
17. Rovira À, Ruiz-Falcó ML, García-Esparza E, López-Laso E, Macaya A, Málaga I et al (2014) Recommendations for the radiological diagnosis and follow-up of neuropathological abnormalities associated with tuberous sclerosis complex. J Neurooncol 118(2):205–223
18. Adriaensen ME, Schaefer-Prokop CM, Stijnen T, Duyndam DA, Zonnenberg BA, Prokop M (2009) Prevalence of subependymal giant cell tumors in patients with tuberous sclerosis and a review of the literature. Eur J Neurol 16(6):691–696
19. Goh S, Butler W, Thiele EA (2004) Subependymal giant cell tumors in tuberous sclerosis complex. Neurology 63(8):1457–1461
20. Roach ES, Williams DP, Laster DW (1987) Magnetic resonance imaging in tuberous sclerosis. Arch Neurol 44(3):301–303

21. Inoue Y, Nemoto Y, Murata R, Tashiro T, Shakudo M, Kohno K et al (1998) CT and MR imaging of cerebral tuberous sclerosis. Brain Dev 20(4):209–221
22. Yates JR, Maclean C, Higgins JN (2011) Tuberous Sclerosis 2000 Study Group. The Tuberous Sclerosis 2000 Study: presentation, initial assessments and implications for diagnosis and management. Arch Dis Child 96(11):1020–1025
23. Nishio S, Morioka T, Suzuki S, Kira R, Mihara F, Fukui M (2001) Subependymal giant cell astrocytoma: clinical and neuroimaging features of four cases. J Clin Neurosci 8(1):31–34
24. Adriaensen ME, Zonnenberg BA, de Jong PA (2014) Natural history and CT scan follow-up of subependymal giant cell tumors in tuberous sclerosis complex patients. J Clin Neurosci 21(6):939–941
25. Altman NR, Purser RK, Post MJ (1988) Tuberous sclerosis: characteristics at CT and MR imaging. Radiology 167(2):527–532
26. Kotulska K, Józwiak S (2012) Subependymal giant cell astrocytoma: role of mTOR pathway and its inhibitors. In: Hayat MA (ed) Tumors of the central nervous system, vol 5. Springer, New York, pp 45–56